frontiers in Marine Science

ORIGINAL RESEARCH
published: 04 December 2018
doi: 10.3389/fmars.2018.00456

Study on Different Fractions of Organic Molecules in the Baltic Sea Surface Microlayer by Spectrophoto- and Spectrofluorimetric Methods

Violetta Drozdowska[1], Piotr Kowalczuk[2], Marta Konik[2] and Lidia Dzierzbicka-Glowacka[1]*

[1] Physical Oceanography Department, Institute of Oceanology, Polish Academy of Sciences, Sopot, Poland, [2] Marine Physics Department, Institute of Oceanology, Polish Academy of Sciences, Sopot, Poland

The sea surface microlayer (SML), created by surface active organic molecules (called: surfactants), is a highly active interface between the sea and the atmosphere. In this study we used the absorption and fluorescence analysis of organic matter collected in the SML and in subsurface layer, of 1 m depth, to describe the changes in molecular size and weight and the composition of surfactants. Data were collected during three research cruises in coastal zone and open waters of the Baltic Sea. The values of the CDOM absorption coefficient were higher in the SML about 29% (in the UV light) to 17% (in a blue spectral range), that reveal dominance of low molecular weighted CDOM molecules, absorbing in the UV light, in the SML. The spectral slope coefficients at different spectral ranges, $S_{\Delta\lambda}$ increased with salinity, while the slope coefficient for 350–400 nm reach lower values by 10.5% in SML compared to SS, caused by an effect of irradiation on the SML. The fluorescence intensities of the main peaks at Excitation Emission Matrix spectra belonging to the main fluorescing components of marine organic matter, called: *A*, *C*, *M*, *T*, were higher in SML by 41, 43, 41, and 14% compared to SS. The ratio of fluorescence intensities, $(M+T)/(A+C)$ and humification index, *HIX*, in the SML were, respectively, higher by 17.9% and lower by 10.7% compared to SS. These relationships reveal more intensive process of *in situ* produced components in the SML as well as faster removal of humic components of high MW in the SML. We have observed an increase of spectral slope ratio, S_R, ($S_{275-295} > S_{350-400}$) with increasing salinity (from 4.5 to 7.94 of practical salinity), being proof that the samples acquire more marine in character. The S_R increased with salinity 33.5 and 23.6% in the SML and SS, respectively, and their maximal values in open water were still maintained. The fluorescence intensity of all FDOM peaks decreased in the same salinity gradient. The decrease rate was higher in SML for the fluorescing peaks by 34, 36, and 26% for *A*, *C*, and *M*, respectively than in the SS. Decrease rate indicated the susceptibility to photochemical degradation of respective peaks. This effect was strongest for C, while T peak was almost unbleached. The fluorescence intensity decrease rate was smaller in SS what indicated shielding effect of the SML.

Keywords: surfactants, fluorescence, absorption, sea surface microlayer, the Baltic Sea, CDOM, FDOM

OPEN ACCESS

Edited by:
Laura Tuomi,
Finnish Meteorological Institute, Finland

Reviewed by:
Manuel Dall'Osto,
Instituto de Ciencias del Mar (ICM), Spain
X. Antón Álvarez-Salgado,
Instituto de Investigaciones Marinas, Spain

****Correspondence:***
Violetta Drozdowska
drozd@iopan.pl

Specialty section:
This article was submitted to Marine Biogeochemistry, a section of the journal Frontiers in Marine Science

Received: *30 April 2018*
Accepted: *13 November 2018*
Published: *04 December 2018*

Citation:
Drozdowska V, Kowalczuk P, Konik M and Dzierzbicka-Glowacka L (2018) Study on Different Fractions of Organic Molecules in the Baltic Sea Surface Microlayer by Spectrophoto- and Spectrofluorimetric Methods. Front. Mar. Sci. 5:456. doi: 10.3389/fmars.2018.00456

INTRODUCTION

The sea surface microlayer (SML), commonly defined as the upper 0–1 mm of the surface ocean (Liss and Duce, 1997) is described by different physical properties than the underlying layers due to the molecules that form the surface film (Hardy, 1982). The SML is almost ubiquitous and covers most of the surface of the ocean, even under conditions of high turbulence (Cunliffe et al., 2013). The SML is created by the surface active organic molecules, called surfactants, characterized by an amphiphilic structure, i.e., with hydrophobic and hydrophilic heads. The hydrophobic properties of the surfactants cause the aquatic environment to push them to the interfacial boundary, to minimize the internal energy of the aqueous system. The SML interacts with the surface accumulation of organic matter produced by biological processes in the underlying water column (Galgani et al., 2016; Kurata et al., 2016). The SML also accumulates a variety of colloidal and particulate organic matter that may be substrates for bacterioneuston, and therefore the SML is called as a complex hydrate "gel" of macromolecules and colloidal material (Sieburth, 1983).

The organic matter in the sea have the allochthonous (from terrestrial input) and autochthonous (derived from primary production in the water column) origin and dissipate due to loss of material at the sea surface by microbial degradation, chemical and photo-chemical processes and loss due to absorption and adsorption onto particles (Aiken et al., 1985; Tilstone et al., 2010; Cunliffe et al., 2011; Cunliffe et al., 2013; Engel et al., 2017). The main mechanism that affects the organic matter in the surface top layer of the ocean is the sunlight. The loss of the color (photobleaching) occurs simultaneously with photochemical modification in the organic molecules. Large organic molecules undergo photochemical and biological degradation, that changes their optical properties and the depth of penetration of solar radiation into the sea, especially in the UV and PAR spectral range. Studies on a role of DOM in limiting the light penetration into the sea (Williamson, 1995; Zepp et al., 1998) and its utilization (Kirk, 1994), reactivity (Williams et al., 2010; Zhang et al., 2013) and transport of inorganic and organic pollutants (Chin et al., 1994; Miller and Zepp, 1995; Stedmon et al., 2003; Pastuszak et al., 2012) are carried out intensively in various marine basins.

The organic matter dynamics are often studied by the changes in chromophoric or fluorophoric fractions of DOM (i.e., CDOM or FDOM) (Boehme and Wells, 2006; Hudson et al., 2007; Cisek et al., 2010; Williams et al., 2010; Drozdowska et al., 2013, 2017). CDOM absorbs light in the UV and visible region and its absorption spectrum decreases exponentially toward longer wavelengths. CDOM participates in various photochemical reactions, including the production of CO and dissolved inorganic carbon (Gao and Zepp, 1998; Szymczycha et al., 2017) and remineralization of terrestrial DOM in a system of the Baltic Sea (Kuliński et al., 2016). The photochemical reactions transform it into smaller and more bio-available forms, and photo-bleaching is recognized as the most important sink for CDOM in the ocean (Zhou and Mopper, 1997; Moran et al., 2000; Goldstone et al., 2004; Zhang et al., 2013; Gonsior et al., 2014; Timko et al., 2015). A specific structure of the energy levels of the complex CDOM molecules results in a specific spectral distribution of the light intensity. Absorption and fluorescence spectra may allow the identification of chromophores and fluorophores belonging to the organic molecules and their sources (Højerslev, 1974, 1988; Coble, 1996; Chari et al., 2012). Changes in the values of the spectral slope coefficients varied inversely proportionally to the CDOM molecular mass (Amon and Budeus, 2003; Twardowski et al., 2004; Helms et al., 2008). According to the experiments carried out by Helms et al. (2008) the values of $S_{275-295}$ and S_R should be higher in the SML due to more effective photobleaching process in the SML. Earlier studies have proposed that the UV-Vis absorption spectra of CDOM at longer wavelengths (>350 nm) originate from a continuum of charge transfer (CT) states between a large number of charge acceptors and charge donors (Del Veccio and Blough, 2004). The absorption at shorter wavelengths, in the UV, should rather be a superposition of discrete chromophores. This suggests a different optical and molecular origin of the absorption signals recorded for the same sample. The UV irradiation influences chromophores, associated with HMW CDOM, and destroys them resulting in a shift from a pool of HMW to LMW of CDOM molecules. Photobleaching process, more effective in the SML, influences the mass balance between high-molecular weighted (HMW) CDOM and low-molecular weighted (LMW) CDOM in the surface layers. The amplitude of $a_{CDOM}(\lambda)$ curve is a proxy for concentration of CDOM, the spectral slope is often used as a proxy for CDOM composition, including the ratio of fulvic to humic acids and molecular weight (Carder et al., 1989; Blough and Green, 1995; Twardowski et al., 2004).

The other method for identification complex and labile organic matter compounds is the fluorescence spectroscopy. Coble (1996) attributed the distinct fluorescence intensity peaks of Excitation Emission Matrix to different types of fluorophores found in natural waters; where peak A (ex./em. – excitation and emission – 250/437 nm) is attributed to terrestrial UV humic like substances; peak C (ex./em. 310/429 nm) represents terrestrial visible-humic like substances; peak M (ex./em. 300/387 nm) characterizes marine humic like substances; and peak T (ex./em. 270/349 nm) represents proteinaceous substances (Zhang et al., 2013). Fluorescence intensities of the main FDOM components: A, C, M, and T (in R.U.) can be used as a proxy of FDOM concentration (Kowalczuk et al., 2005; Loiselle et al., 2009; Drozdowska and Fateyeva, 2013; Drozdowska and Józefowicz, 2015; Drozdowska et al., 2017). Additionally, several fluorescing indices help in describing the FDOM sources. The humification index, *HIX*, reflects the structural changes that occurred during the humification process, causing an increase in both aromaticity (the ratio C/H) and condensation in DOM molecules (Williams et al., 2010; Chen et al., 2011; Chari et al., 2012). Another fluorescent index allowing description of the DOM composition and source is the $(M + T)/(A + C)$ ratio.

The absorption and fluorescence spectra allow the identification of the sources of organic matter. Additionally, several absorption ($S_{\Delta\lambda}$ in different spectral ranges and a slope ratio) and fluorescence (the ratio of the fluorescence intensities $(M + T)/(A + C)$ and *HIX*) indices help in describing the

changes in molecular size and weight as well as in composition of organic matter.

The Baltic Sea is semi-enclosed sea with the limited water exchange with the Atlantic through the Danish Straits and it has unique optical properties because of a very high input of fresh water from the large surrounding drainage area (Lepparanta and Myrberg, 2009). Previous studies proved that the optical properties of the Baltic Sea water are determined to a large extent by light absorption by CDOM (Højerslev, 1989). Maximum freshwater runoff occurs in April/May and coincidents with phytoplankton blooms. In the winter, wind-driven mixing leads to the vertical thermohaline circulation that reduce biological activity and riverine outflow and results in clearer surface waters (Olszewski et al., 1992; Kowalczuk, 1999; Kowalczuk et al., 2010). CDOM has a significant influence on the spectral properties of the apparent optical properties of the Baltic Sea water (Darecki et al., 2003; Kowalczuk et al., 2005).

Absorption and fluorescence investigations, presented herein, included the open and coastal regions of the Baltic Sea. Measurements were carried out along the transect from the Vistula river outlet to the open sea (Gdansk Deep) and along the transect running across the Baltic Proper, on the section from the Arkona Basin to the Gdansk Deep, i.e., in a coastal zone as well as far from the estuaries and lands. The fluorescence and absorption measurements of the samples collected from a SML and sub-surface layer (SS), at a depth of 1 m, during three research cruises in the Baltic Sea were carried out on 'raw' and filtered samples, to test how the filtration process affects the results of surfactant concentration and composition. One of the main goals of our work is to characterize the specific luminescent properties of molecules present in the SML. While the SML is a complex of dissolved and colloidal and particulate organic matter (Sieburth, 1983) the filtration process was omitted in a part of our laboratory procedures, so as not to get rid of the essential ingredients of the "gel."

The authors have conducted research on the SML properties in the several estuaries of the southern Baltic Sea for almost 10 years (Drozdowska et al., 2013, 2015, 2017; Drozdowska and Józefowicz, 2015). But the results concerned the coastal zone only. The new dataset, as the results from the cruises in 2015 and 2016 concerning spatially and hydrological diverse areas, prompted us to perform comparative analyzes of the results. The objectives of the research is to determine what physical parameters of the environment affect the composition of surfactants, where there is no significant impact of rivers. The main objectives are (i) to detect any changes in surfactant concentration and composition in the open sea and in coastal waters and which components predominate in open water; (ii) to evaluate/estimate differences in spectroscopic properties performed on 'raw' and filtered samples.

MATERIALS AND METHODS

Field Works and Sampling

Sampling of the seawater probes for studying the absorption and fluorescence properties of organic matter in the SML and SS were carried out during three cruises: one in a summer (7–10 June) 2015 on a board of R/V Academik Ioffe, and two in an autumn 2016 on R/V Oceania (**Figure 1**). During the research cruise in June 2015, sampling was made on 25 stations, across the transect through the Baltic Proper from the Arkona Basin through Bornholm Basin and Slupsk Furrow to the Gdansk Deep. The ship was slowing down on the stations allowing the surface water to be collected into the wide container. Next, after 15 min, the newly formed SML was collected by the Glass Plate (Falkowska, 1999). The collected samples were prepared to laboratory measurements. The samples collected on the first three stations, on 7 June, were frozen, while the next samples (collected in 8–10 June) were put to a refrigerator and were analyzed immediately after the end of the cruise in a lab, within 48 h after sampling. During two research cruises in 2016: on 24 September and 2 November, samplings were conducted across the transect from the Vistula River outlet, to the open waters in Gdansk Deep. The seawater samples from SML were collected by the Garrett Screen (Garrett, 1965; Carlson, 1982), mesh 18. The screen was firstly immersed in the water, parallel to the sea surface, to stabilize the surface microfilm and carefully raised in a horizontal position. Then water was poured to a polyethylene bottle. In September and November' 2016, the samples from the SS, using a Niskin bottle, were taken as well. Sampling by stainless-steel Garrett Screen, GS, yields the collection of a relatively thick layer compared to Glass Plate, GP, sampling technique, which may cause the differences in the results. However, screen samples are characterized by a higher degree of dilution with underlying water, hence the quantity of organic molecules is rather representative for the thinner thickness of the water layer. Additionally, the results of absorption and fluorescence measurements concerning the station in the open Baltic Sea, collected by GP on R/V Akademik Ioffe, do not differ from those concerning the last station of the transect V (at the Gdansk Deep) by GS on R/V Oceania. Each time about 1 L of the SML water was collected. Sampling during the cruises in 2016 were done at the last day of the cruise and the lab analyses were performed at the next day, so within 24 h after sampling. The part of water samples were passed through Sartorius 0.2 μm pore cellulose membrane filters to remove bigger and fine-sized particles. The 'raw' and filtered water samples were stored in the dark at 4°C until analysis in the land-based laboratory. On every station during the cruises the hydrographic data, of the upper layer of 1 m, were recorded; on R/V Akademik Ioffe by a Idronaut 320+ while on R/V Oceania with a SeaBird SBE 911+ CTD system. Moreover the meteorological observations were made to control the state of the sea, and during our experiments sea state was beneath 4B and a lack of the precipitation.

Laboratory Measurements

Spectrophotometric and spectrofluorometric measurements of seawater samples were performed in the laboratories of the Institute of Oceanology, the Polish Academy of Sciences. Before any spectroscopic measurements, the water samples were left to warm up to room temperature. The absorption and fluorescence analysis were performed on the 'raw' and filtered samples, except for a summer' 2015, when the fluorescence measurements

were performed on the 'raw' samples only. During the other experiments the measurements on 'raw' and filtered water samples from the SML and SS were carried out simultaneously.

Absorption Measurements and Absorption Indices

CDOM absorption spectra were measured on Perkin Elmer Lambda 650 spectrophotometer in the spectral range 240–700 nm. For measurements the quartz 10 cm cuvettes were used and an ultrapure Milli-Q water was used as a reference signal. The recorded absorbance $A(\lambda)$ spectra were processed to get the curves of the CDOM absorption coefficients $a_{CDOM}(\lambda)$, m^{-1}. Next, a non-linear least-squares fitting method was applied (Stedmon et al., 2000; Kowalczuk et al., 2006) to calculate the spectral slope coefficient, $S_{\Delta\lambda}$, in the several spectral ranges: 275–295 and 350–400 nm, $S_{275-295}$ and $S_{350-400}$, respectively. The dimensionless parameter called "a slope ratio," S_R, as a ratio of two spectral slope coefficients, $S_{275-295}$ and $S_{350-400}$, was calculated as well. The detailed procedure is described in the papers by Kowalczuk et al. (2009) and Drozdowska et al. (2017).

Fluorescence Measurements and Fluorescence Indices

The 3D-fluorescence spectra (EEM) were carried out on Varian Cary Eclipse scanning spectrofluorometer in a 1 cm path length quartz cuvette using a 4 mL sample volume. Series of emission scans (280–600 nm at 2 nm resolution) over an excitation wavelength range from 250 to 500 nm at 10 nm increments were measured. The instrument was configured to collect the signal using maximum lamp energy and 5 nm band pass on both the excitation and emission monochromators. The results of fluorescence measurements were not corrected by the inner filter effect that may lead to the re-absorption of the emitted light (for the samples with CDOM absorption coefficient $> 10\ m^{-1}$). To normalize the EEM spectra of seawater samples, the fluorescence EEM spectrum of Milli-Q water, as a blank sample, was measured using the same instrumental set-up. The intensity of the Milli-Q water Raman signal, as the integral in the spectral range: 374–424 nm of the Raman emission spectrum, exited at 350 nm, (Murphy et al., 2010) was calculated. The blank Milli-Q EEM spectrum was subtracted from the all EEM spectra of seawater samples. Then all blank corrected EEMs of seawater sample spectra were normalized to Milli-Q water Raman emission [scaled to Raman units (R.U.)] by dividing the resulting spectra by calculated Raman emission intensity value. The procedure is described in details in the literature (Drozdowska et al., 2013, 2017).

The humification index, *HIX*, is calculated as a ratio of two fluorescence bands, in the near-visible and UV-A range of the fluorescence spectrum excited at 255 nm (Zsolnay et al., 1999; Glatzel et al., 2003). That is a ratio of a fluorescence intensity at a blue-part of the spectrum, at: 435–480 nm to a fluorescence intensity at the UV-A part: 330–346 nm. *HIX* is directly proportional to the humic content of DOM, where *HIX* values around 1–2 are associated with non-humified plant materials while values >10 are commonly reported for fulvic acid extracts (Zsolnay et al., 1999; Williams et al., 2010).

The fluorescent index, the $(M + T)/(A + C)$ ratio, allows description of the DOM composition and source. The $(M + T)/(A + C)$ ratio is a derivative of the β/α ratio, proposed by Parlanti et al. (2000); where β region, the emission at 380 nm, is divided by α region, the emission band between 420 and 435 nm – for excitation at 310 nm. The fluorescence intensities, ratio, $(M + T)/(A + C)$, allows the assessment of the relative contribution of dissolved organic matter recently produced *in situ*, M and T, to humic substances characterized by highly complex high-molecular-weighted (HMW) structures, A and C (Parlanti et al., 2000; Osburn et al., 2009; Wilson and Xenopoulos, 2009; Williams et al., 2010; Drozdowska et al., 2015). Values of the ratio >1 indicate the predominant amount of autochthonous DOM molecules, while values of <0.6 indicate the allochthonous ones (Huguet et al., 2009). The $(M + T)/(A + C)$ ratio is correlated positively with bacterial production of terrestrial DOM and indicate the presence of microbially derived DOM (peak T) in aquatic ecosystems (McKnight et al., 2001). Additionally, the ratio is well-correlated with a photobleaching and points to a decrease in terrestrial components (A and C) decomposed by the irradiation (Williams et al., 2010).

RESULTS

Analysis of the Absorption Data

The absorption spectra recorded for the samples collected from the SML and SS during three Baltic cruises show the differences in the slope of the curves as well as in the values of the spectral distribution of the absorption coefficient for different seasons and studied areas. The lowest values of CDOM absorption coefficient were recorded for the Baltic Proper, in June, due to the largest distance from lands and river outflows and in November, due to low biology activity and reduced river water inflows. The CDOM absorption coefficient recorded for 'raw' and filtered samples at the same station show higher values for 'raw' samples, with the exception for short-UV spectral region, where the higher values are reached for the filtered samples. Moreover, the curves of the spectral resolution of the CDOM absorption coefficient for the samples collected at the very mouth of the river have less inclined shape, what means a presence of a greater amount of components absorbing at longer wavelengths, 300–400 nm (Grzybowski, 2000; Twardowski et al., 2004; Helms et al., 2008).

Figure 2 presents the relation between salinity and CDOM absorption coefficient at several wavelengths for 'raw' and filtered samples collected from the SML and SS during Baltic cruises. The graph shows the decrease of CDOM absorption coefficient, along with an increase in salinity. As one can see, the CDOM absorption coefficient decreases and the fastest decrease (the highest value of a linear regression coefficient) occurs at the UV range, wavelengths 254 nm, while the slowest one at the longer wavelength, 410 nm, in both SML and SS (Twardowski et al., 2004; **Table 1**).

The CDOM absorption coefficient has lower values for filtered waters in the entire examined light spectrum. The wavelength

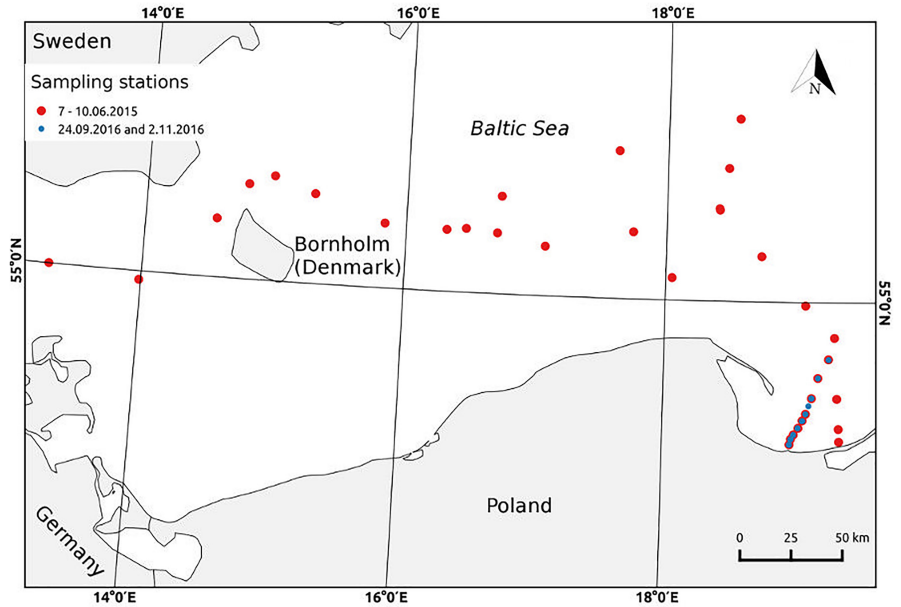

FIGURE 1 | Map of sampling stations during the cruises in June' 2015, on R/V Akademik Ioffe (red dots) and in September and November' 2016 on R/V Oceania (blue dots).

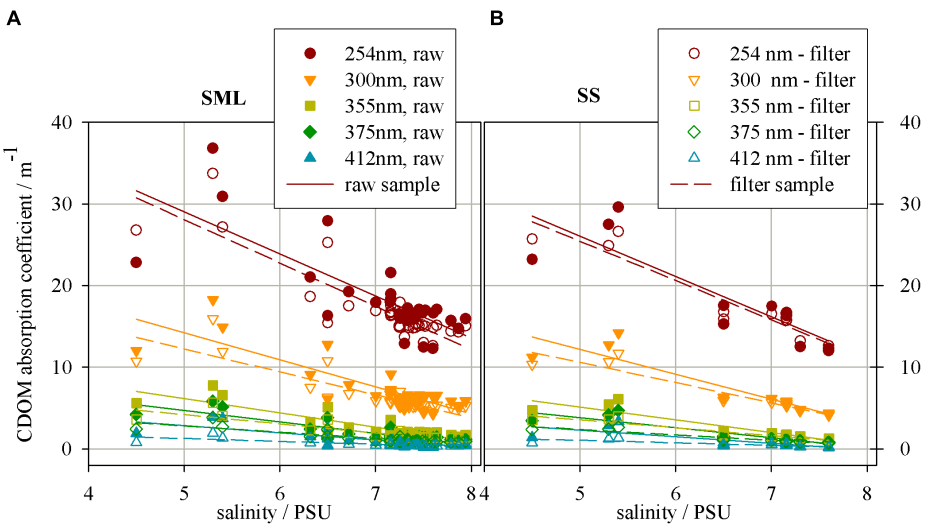

FIGURE 2 | The relation between salinity and CDOM absorption coefficient in different wavelength for the samples collected from **(A)** a surface microlayer (SML) and **(B)** a depth of 1 m (SS), for 'raw' and filtered samples.

254 nm was chosen due to specific electron transition occuring in the region of the UV range, for some aromatic hydrocarbons. These molecules are the precursor for components of certain types of humic substances (particularly those derived from terrestrial sources).

Differences between the values of regression coefficients between SML and SS as well as filtered and 'raw' samples are clearly visible (see **Table 1**). However, due to the uncertainty (standard deviations) of the obtained regression coefficients, it was necessary to check the hypothesis that these coefficients are significantly different. We put the null hypothesis H_0 that the coefficients are equal and tested this hypothesis. Significance tests were calculated for the linear correlations between salinity and the values of CDOM absorption coefficient yielded for different samples. The significant ratio, SR, was calculated as follows:

$SR = |a_1 - a_2|/\sqrt{(S_{a_1})^2 + (S_{a_2})^2}$; where a_1 and a_2 – regression coefficients of the two relations, S_{a_1} and S_{a_2} – the standard deviation of the regression coefficients. If $SR > 1.96$ it means that we can reject the hypothesis H_0 that the regression coefficient are equal at $P < 0.05$.

TABLE 1 | The relation between salinity and the CDOM absorption coefficients (**Figure 2**).

For $a_{CDOM}(\lambda)$	Linear regression coefficients between $a_{CDOM}(\lambda)$ and salinity; $a_{CDOM}(\lambda) = a \cdot Salinity + b$					
	a (Sa)	b (Sb)	r^2	a (Sa)	b (Sb)	r^2
λ/nm	SML – 'raw' samples			SML – filtered samples		
254	−5.13 (0.73)	54.68 (5.24)	0,54	−5.31 (0.50)	54.6 (3.6)	0,76
300	−3.32 (0.38)	30.82 (2.7)	0,67	−2.81 (0.29)	26.25 (2.05)	0,73
355	−1.76 (0.17)	14.96 (1.24)	0,74	−1.13 (0.11)	9.86 (0.81)	0,74
375	−1.4 (0.14)	11.69 (0.99)	0,73	−0.87 (0.078)	6.71 (0.56)	0,75
412	−0.89 (0.12)	7.29 (0.89)	0,55	−0.35 (0.053)	3.01 (0.38)	0,55
λ/nm	SS – 'raw' samples			SS – filtered samples		
254	−4.93 (0.77)	50.67 (5.25)	0,76	−4.82 (0.42)	49.5 (2.84)	0,91
300	−3.05 (0.37)	27.49 (2.53)	0,84	−2.48 (0.24)	23.02 (1.62)	0,89
355	−1.56 (0.19)	12.89 (1.29)	0,84	−0.97 (0.09)	8.39 (0.63)	0,89
375	−1.23 (0.16)	9.99 (1.1)	0,82	−0.67 (0.062)	5.72 (0.42)	0,9
412	−0.79 (0.17)	6.21 (1.16)	0,62	−0.31 (0.06)	2.56 (0.38)	0,69

Firstly, the calculations of the H_0 were made for the absorption results. The values of *SR* referring to the differences between the regression coefficients for filtered and 'raw' samples, for the SML or SS separately, are <1.96 in the UV spectral range, in both layers. Thus, the differences between filter and 'raw' samples are at the UV light (254 and 300 nm) statistically irrelevant. The values of *SR*, are >1.96 at blue/visible light (355, 375, and 412 nm), that support the significant differences between filtered and 'raw' samples, both in the SML and SS. Next, the tests of significant differences for the regression coefficients for the SML and SS samples were calculated, for the filtered and 'raw' ones separately. The *SR* is about 1 (less than 1.96) in the all spectral range, so the differences between the regression coefficients for the SML and SS are irrelevant at $P < 0.05$, for both, the filter and 'raw' samples.

Analysis of the Fluorescence Data

Studies on 3D fluorescence spectra allowed following changes in the intensity of emission bands belonging to the fluorophores A, C, M, and T. Peak intensity values (in R.U.) of the fluorescence bands of the basic FDOM components decreased with increasing salinity both in the SML and SS, **Figures 3A** and **B**, respectively. The linear regression coefficients of the relation between fluorescence intensity and salinity reach higher values in the SML waters than SS. The values of linear regression analysis are included in **Table 2**. The analysis of fluorescence spectra also allowed following the changes in the percentage composition of the main components of FDOM (in %) occurring in SML and SS, as shown in **Figures 3C** and **D**, respectively. A percentile contribution of the main FDOM fluorophores, calculated as the ratio of the respective peak intensity (A, C, M, or T) to the sum ($A + C + M + T$) of all peak intensities, gives information about the relative changes of a fluorophore composition in a sample. Changes in the share of individual components in the SML and SS, both in 'raw' and filtered samples, are presented in **Figure 3**.

It can be seen that the fluorescence intensity of a component A decreases faster then C and next M, while T component decreases the most slowly with an increase of salinity (their regression coefficients, a, are as follow: −0.47, −0.3, −0.19, and −0.06 for the SML and −0.35, −0.22, −0.15, and −0.06 for the SS, respectively). All linear regression coefficients were higher in the SML except of T component, for which they were similar in both layers, for both 'raw' and filtered samples (**Table 2**, **Figures 3A**, **B**). Moreover, the percentile composition of the main FDOM components in 'raw' samples in the SML shows that the share of components A and M is almost constant, only C decreases and T increases with salinity. While, in SS the share of components A, M, and C almost do not change throughout the studied area, while T increases (**Figures 3C,D**).

Due to the standard deviations of the regression coefficients, put in **Table 2**, it is necessary to check the hypothesis that the regression coefficients for different relations are significantly different. The values of the *SR* calculated for the differences between the regression coefficients for filtered and 'raw' samples, in the SML and SS separately, show that $SR < 1.96$ in the all fluorescent components (i.e., A, C, M, and T). Thus, the differences between the regression coefficients for filter and 'raw' samples, are statistically insignificant. Next, the tests of significant differences between the regression coefficients between the SML and SS samples, were calculated, for the filtered and 'raw' ones separately. The *SR* ratio oscillate between 1.23–1.79, except the component T (0.23–0.41). Thus, the values of $SR < 1.96$, so the differences between the regression coefficients for the SML and SS are insignificant for both, the filter and 'raw' samples at $P < 0.05$.

Analysis of the Absorption Indices

Figure 4 shows the values of the slope coefficients, $S_{275-295}$ and $S_{350-400}$ (in nm^{-1}) in different wavelength ranges, respectively: 275–295 nm, 350–400 nm as well as the dimensionless parameter called "a slope ratio," S_R. The slope ratio coefficient, as the ratio of two spectral slope coefficients, $S_{275-295}$ and $S_{350-400}$,

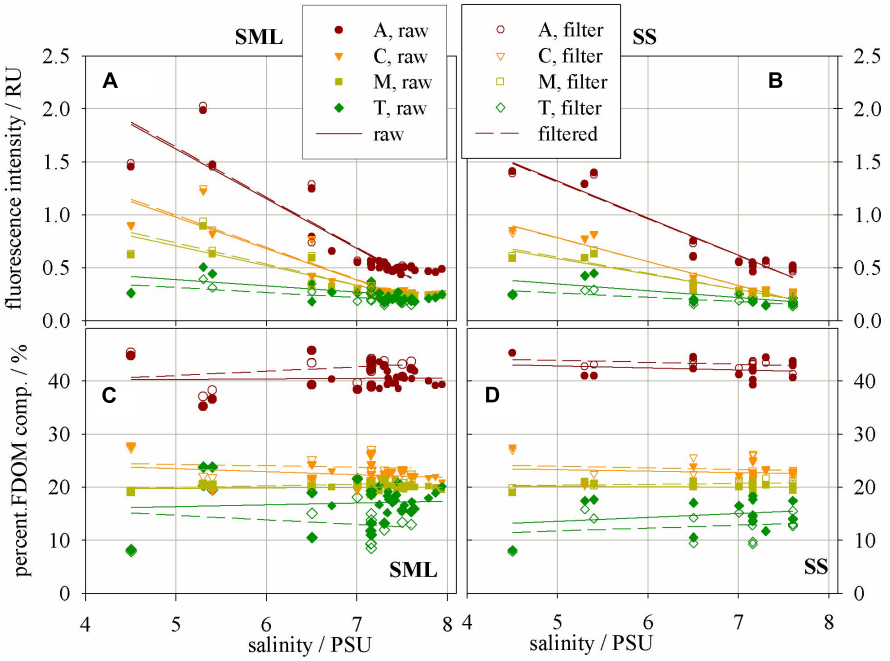

FIGURE 3 | Fluorescence intensity – a proxy of concentration of fluorophores – the main FDOM components in **(A)** SML and **(B)** SS; Percentage composition of the main FDOM components in **(C)** SML and **(D)** SS.

TABLE 2 | The relation between salinity and the fluorescence intensities of FDOM components (**Figure 3**).

Linear regression coefficients between FDOM component and salinity; *fl.intens.*(*FDOM comp.*) = *a* · *Salinity* + *b*						
	a (Sa)	**b (Sb)**	r^2	**a (Sa)**	**b (Sb)**	r^2
FDOM component	**SML – 'raw' samples**			**SML – filtered samples**		
A	−0,47 (0.066)	3.97 (0.45)	0,81	−0,47 (0.07)	4.0 (0.46)	0,80
C	−0,30 (0.043)	2.46 (0.29)	0,80	−0,3 (0.04)	2.51 (0.3)	0,80
M	−0,0.19 (0.03)	1.64 (0.21)	0,75	−0,20 (0.03)	1.73 (0.23)	0,74
T	−0,0.06 (0.027)	0.68 (0.18)	0,28	−0.05 (0.018)	0.55 (0.12)	0,37
FDOM component	**SS – 'raw' samples**			**SS – filtered samples**		
A	−0,35 (0.031)	3.07 (0.21)	0,91	−0,35 (0.03)	3,05 (0.19)	0,93
C	−0,22 (0.02)	1.91 (0.13)	0,91	−0,22 (0.02)	1,9 (0.13)	0,92
M	−0,15 (0.013)	1.31 (0.09)	0,90	−0,15 (0.015)	1,37 (0.1)	0,89
T	−0.064 (0.018)	0.67 (0.12)	0,49	−0.04 (0.008)	0,47 (0.05)	0,68

TABLE 3 | The equations related to **Figure 4**.

$a_{CDOM}(\lambda) = 2.303 \times A(\lambda)/l$ $A(\lambda)$ – the corrected spectrophotometer absorbance at wavelength λ l – the optical path length [m]; quartz cuvette – 10 *cm*	Eq. 1
The CDOM absorption curve: $a_{CDOM}(\lambda) = a_{CDOM}(\lambda_0)e^{S(\lambda_0-\lambda)} + K$, $\lambda_0 - 350\,nm$, K – background constant, S and K – estimated simultaneously via non-linear regression using Eq. 2 in the spectral range (300–600 nm)	Eq. 2
Linear regression coefficients between the slope coefficient, S, in different ranges, $\Delta\lambda$, and salinity: $S_{\Delta\lambda} = a \cdot Salinity + b$	Eq. 3

is calculated for the SML and SS. The values of the all slope factors increase with increasing salinity. The values of the spectral slope coefficients in the range 275–295 and 350–400 nm increase with salinity, while in the UV range faster, both in 'raw' and filtered samples in the SML and SS. It occurs under the irradiation causing increasing of $S_{275-295}$ and decreasing of $S_{350-400}$. Generally, during irradiation chromophores associated with HMW CDOM are destroyed during photobleaching process that

gives result in a shift of a significant portion of CDOM molecules from HMW to LMW phase (**Figures 4A**,**B**). In the SML the values of $S_{275-295}$ and $S_{350-400}$ (in nm^{-1}) change in a range 0.0093 to 0.0218 and 0.0085 to 0.019, respectively, while in the SS they change in the ranges: 0.010 to 0.022 and 0.009 to 0.0171, respectively. In the filtered samples the values of spectral slope coefficients in the SML and SS are closed to each other. The values of the spectral slope coefficient $S_{275-295}$ in filtered samples change in the range 0.0178 to 0.0243 and from 0.0192 to 0.0236 for the SML and SS, respectively, while a coefficient $S_{350-400}$ changes in the ranges 0.0171 to 0.0.0233 and 0.0171 to 0.0226 in the SML and SS, respectively. Thus, the changes of a spectral slopes in the study area, with salinity, for the 'raw' samples yielded about 100%, while in the filtered ones 25–35% only, both in the SML and SS.

The results of S_R both in the 'raw' and filtered samples give the values >1, that means a near shore (marine-like) character of the samples (Helms et al., 2008). What is more, the values of S_R in 'raw' samples change in a range from 1.093 to 1.513 and from 1.145 to 1.485 in the SML and SS, respectively. While the ranges of the values of S_R in the filtered samples for the SML and SS are much narrower and the range limits lay close to each other, from 1.029 to 1.3737 for the SML and from 1.027 to 1.269 for the SS. However, the percentile changes of MW in the SML and SS reflected by S_R yield 33.5 and 23.6% for filtered water, respectively and 38.5 and 29.6% for 'raw' ones. Thus, the changes of MW between the SML and SS, both for filtered and 'raw' samples, reveal about 10% and the changes are related to shift in molecular weight caused by photobleaching in the SML.

Analysis of the Fluorescence Indices

The **Figure 5** presents the humification index as well as the ratio of fluorescence intensities at peaks of the main FDOM components in the SML and SS (**Figures 5A** and **B**, respectively), as the results of the degradation processes. The values of *HIX* index are smaller in 'raw' samples, which means that the denominator has a higher value (more component T in 'raw' than in filtered samples). The humification index, *HIX*, changed in the SML in a range from 3.8 to 17.9, while in the SS it ranged from 6.09 to 18.68. *HIX* index achieved a little higher values in the SS than in the SML. Additionally, *HIX* index achieved higher values for both, SML and SS, for filtered samples. The one exception, for filtered samples, are the results obtained for the station at the very mouth of the river. On the graphs on **Figure 5** the changes of the ratio of the fluorescence intensities of FDOM components created in the sea, M and T, to the sum of fluorescence intensity of the components brought in by rivers, A and C, are presented as well. The values of the ratio $(M + T)/(A + C)$, for 'raw' samples, vary in the SML in a range 0.39 to 0.8 while in the SS from 0.36 to 0.63. The results obtained for filtered ones in the SML varied in a range: 0.38 to 0.69,

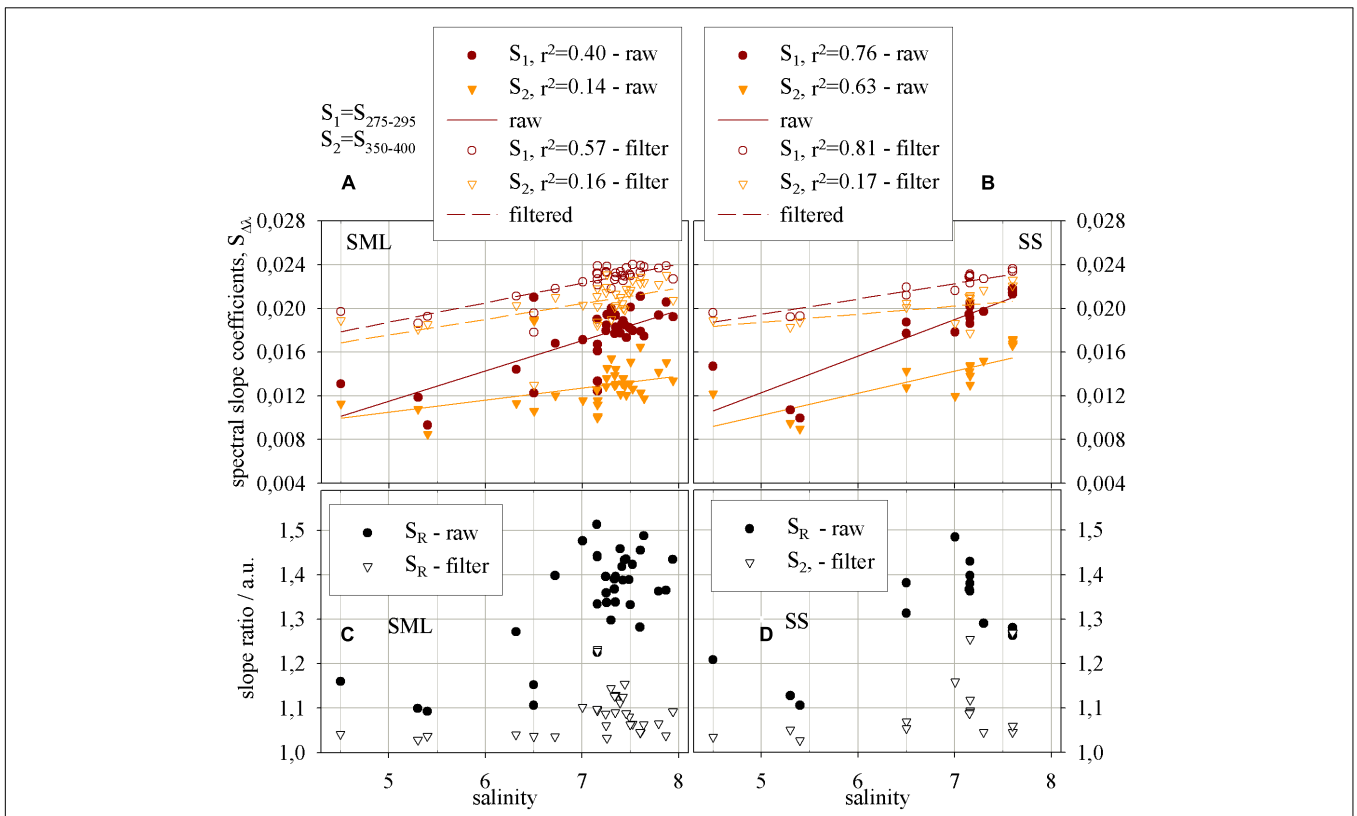

FIGURE 4 | The relations, for the SML and SS, respectively, between salinity and **(A,B)** the spectral slope and **(C,D)** the slope ratio coefficients. Spectral slope coefficients increase (i.e., molecular weight decreases) with raising salinity, for 'raw' and filtered samples, in **(A)** the SML and **(B)** SS. The report of the equations applied to reach the results presented on the graphs – **Table 3**.

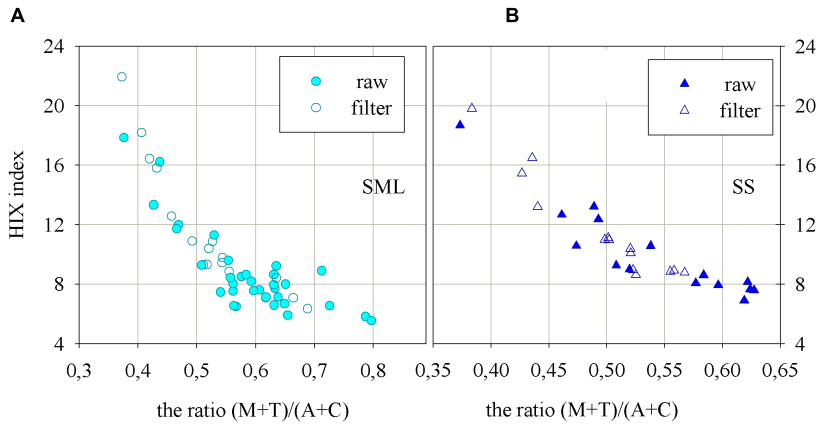

FIGURE 5 | The relation between the ratio of fluorescence intensities of the main components of FDOM, $(M + T)/(A + C)$, and humification index, *HIX*, for the **(A)** SML and **(B)** SS water.

while in the SS: 0.38 to 0.58. The results of the ratio of the fluorescence intensities show higher values in the SML than in the SS and a little higher values in the 'raw' samples than in filtered ones.

DISCUSSION AND CONCLUSION

Our experimental results address two aspects of surfactant photochemistry in brackish sea environments: (i) the influence of photochemical processes on terrestrially derived light-absorbing and fluorescing material resident in the study aquatic system and (ii) what corrections and changes are made by using the 'raw' and filtered water samples when studying the properties and concentrations of surfactants (the molecules of surface-active organic matter).

The CDOM absorption coefficients as well as the fluorescence intensity of FDOM components decrease with increase of salinity. The decrease of the values of the CDOM absorption coefficient reveals the fastest decrease (the highest value of a linear regression coefficient) at the UV range, at the wavelength 254 nm, while the slowest one at the longer wavelength, 410 nm, in both SML and SS. In the UV range some aromatic hydrocarbons, that are the precursor for components of terrestrial humic-like substances, absorb. The highest decrease of the fluorescence intensity of the main FDOM components occurred for a UV-absorbing terrestrial humic-like, component A, then a visible-absorbing terrestrial humic-like, component C, and the slowest decrease for marine humic-like component, M. While protein-like component, T, stayed almost unbleached through the all salinity gradient. The results of fluorescence measurements should be corrected using the inner filter effect that may cause the re-absorption of the emitted light by organic matter in the samples characterized by the CDOM absorption coefficient >10 m^{-1}. However, the inner filter correction was not applied and this can affect the fluorescence of peaks A and T in three stations near the mouth of the Vistula. The regression coefficient for the relation between salinity and the fluorescence intensities of the FDOM components indicate higher values in the SML then in SS. The organic molecules of terrestrial origin are decomposed under the influence of the light more effectively (Chin et al., 1994; Chen et al., 2011; Zhang et al., 2013).

Our studies indicate that photochemical processes that affect the surface ocean, observed during a day-light period (either low-intensity or high-intensity irradiance) more efficiently remove colored and fluorescent components from DOM pool in the SML than SS, like it was explored by Moran et al. (2000). The results confirm the dominant share of the terrestrial humic-like molecules in the all studied area, especially in the SML, also in the open surface waters of the Baltic Sea.

The analysis of absorption data allows concluding that the magnitude of absorption coefficient (molar absorptivity) in the UV is indicative of both the degree of humification that has occurred and the contribution of terrestrial materials present in the organic matter sources (Tilstone et al., 2010). The relative amount of aromatic moieties in aquatic fulvic acids increases with increasing molecular weight (Chin et al., 1994; Chari et al., 2012). The analysis of the slope factors of the $a_{CDOM}(\lambda)$ curve, which change inversely proportional to the molecular mass of the absorbing molecules, indicates the presence of DOM molecules with lower molecular weight in the SML than in SS in the all studied regions of the Baltic Sea.

The analysis of the EEM spectra indicates the higher intensities in the fluorescence spectra for the SML than SS samples. Additionally, the most dynamic portion of the absorbing and fluorescing organic matter are the components C and T, that has been previously attributed to fluorescence from terrestrial humic-like material and aromatic amino acids, respectively (Coble, 1996). The explanation of such changes in C component is a photobleaching process, because C fluorophore is in somewhat more susceptible to photochemical degradation than A and M fluorophores (Moran et al., 2000). An increase in amino acid fluorescence (peak T) indicates probably that bacterial transformation of non-photodegradable estuarine DOM can be a source of new fluorophores. T fluorophores also appeared to

be less susceptible to photodegradation (Moran et al., 2000). The elevated values of humification index, *HIX*, in the SS indicate presence of molecules of higher molecular weight that are more condensed, with higher aromaticity, in the SS than in the SML. The ratio $(M + T)/(A + C)$ indicates higher values in the SML because of the bigger amount of T component and lower amount of terrestrial humic substances disintegrated using photobleaching process in the SML (Williams et al., 2010). What is more, the values of the ratio $(M + T)/(A + C)$ are <1, that indicates the significant participation of allochthonous DOM molecules in the SML, even in the open waters of the Baltic Sea.

Humification index, *HIX* is well-related to the ratio $(M + T)/(A + C)$, and in proportional dependence to the terrestrial constituents of organic matter as well. Humification index, *HIX* well-correlates with concentration of terrestrial DOM, means that much of stream DOM in the studied areas of the Baltic Sea originated from humic-like terrestrial material, similarly like it was reported for a lake water (Williams et al., 2010).

The filtering process slightly affects the results of absorption measurements by lowering the $a_{CDOM}(\lambda)$ values of the filtered samples, except for the UV region, and by changing the shape of the curve. The reason of the weak signal in 'raw' samples in the UV may result from the biology processes of living organisms due to disintegration of absorbing aromatic particles by, i.e., fungi, active in degradation and mineralization of humic substances contained in 'raw' samples (Khundzhua et al., 2013). Anyway, the differences between the absorption spectra of the 'raw' and filtered samples occur mainly in the short UV spectral range only. However, these differences do not cause significant changes in the absorption indices, because they are calculated on the basis of the shapes of the spectra (in other words: are based on the relative differences between the values of CDOM absorption coefficient in the central part of the measuring range (Grzybowski, 2000; Twardowski et al., 2004; Helms et al., 2008). The absorption coefficient has higher values for 'raw' samples in both the SML and SS. While, the filtration process almost does not affect the decrease rate of fluorescence intensities, with the exception of T component. The differences between EEM spectra recorded for 'raw' and filtered samples in the studied fluorescence spectra lay in the region of T component mainly. The protein-like molecules, T component, recently produced in the sea in biological and photodegradation processes are the main component of the "gel" and the most effectively retain on the filter. Additionally, the filtration process influences the percentile composition of A and T in the SML, while in the SS it does not play any role.

The analysis of the slope factors of the $a_{CDOM}(\lambda)$ curve, which are inversely proportional to the molecular mass of the absorbing molecules, indicates the presence of lower MW CDOM and little differentiated molecules in filtered samples. While, in the 'raw' samples there were both HMW molecules in areas of low salinity and a LMW ones in the open sea. The *HIX* index achieved a little higher values in filtered samples, while the ratio $(M + T)/(A + C)$ reached lower results in the filtered ones. Thus, the absorption and fluorescence indices show sensitivity to the filtration, due to the presence of molecules with high molecular mass and complex hydrate "gel" ones or lack thereof in the SML.

The results of marine measurements carried out in coastal and open waters of the Baltic Sea constitute a continuous and consistent sequence of data describing absorption and fluorescence properties of marine surfactants. The quantities describing surfactants, studied in the Gulf of Gdansk and Gdansk Deep and in the Baltic Proper, confirm the dominant share of the terrestrial humic-like molecules in the all studied regions of the Baltic Sea. Moreover, the results obtained at the most saline and distant from land-based sources and shoreline, maintain their almost invariable values in the all open waters. Finally, the authors concluded that the degradation processes of the organic molecules contained in the SML and SS proceed at different rates. Hence, the DOM molecules included in the SML may specifically modify the physical processes associated with the sea surface layer.

AUTHOR CONTRIBUTIONS

VD designed the experiments, performed the field and laboratory works, and wrote the paper. PK provided laboratory instrumentation for spectroscopic analysis, gave scientific guidance, and contributed to the paper. MK and LD-G contributed to data analyzing of the laboratory data. All authors reviewed and commented on the paper.

FUNDING

This work was partly supported by Institute of Oceanology Polish Academy of Sciences and the National Centre for Research and Development within the BIOSTRATEG III (Program No. BIOSTRATEG3/343927/3/NCBR/2017).

ACKNOWLEDGMENTS

The authors thank to the scientific team of the research vessels MS Akademik Ioffe and MS/Y Oceania.

REFERENCES

Aiken, G. R., McKnight, D. M., Wershaw, R. L., and MacCarthy, P. (1985). *Humic Substances in Soil, Sediment and Water: Geochemistry, Isolation and Characterization*. New York, NY: Wiley-Lnterscience. doi: 10.1029/2002JC001594

Amon, R. M. W., and Budeus, G. (2003). Dissolved organic carbon distribution and origin in the Nordic Seas: exchanges with the Arctic Ocean and the North Atlantic. *J. Geophy. Res.* 108:3221. doi: 10.1029/2002JC001594

Blough, N. V., and Green, S. A. (1995). "Spectroscopic characterization and remote sensing of nonliving organic matter," in *Role of Nonliving Organic Matter in the Earth's Carbon Cycle*, eds R. G. Zepp and C. Sonntag (New York, NY: Wiley), 23–45.

Boehme, J., and Wells, M. (2006). Fluorescence variability of marine and terrestrial colloids: examining size fractions of chromophoric dissolved organic matter

in the Damariscotta River estuary. *Mar. Chem.* 101, 95–103. doi: 10.1016/j.marchem.2006.02.001

Carder, K. L., Steward, R. G., Harvey, G. R., and Ortner, P. B. (1989). Marine humic and fulvic acids: their effects on remote sensing of ocean chlorophyll. *Limnol. Oceanogr.* 34, 68–81. doi: 10.4319/lo.1989.34.1.0068

Carlson, D. J. (1982). A field evaluation of plate and screen microlayer sampling techniques. *Mar. Chem.* 11, 189–208. doi: 10.1016/0304-4203(82)90015-9

Chari, N. V., Sarma, H. K., Pandi, S. R., and Murthy, K. N. (2012). Seasonal and spatial constraints of fluorophores in the Midwestern Bay of Bengal by PARAFAC analysis of excitation emission matrix spectra. *Estuar. Coast. Shelf Sci.* 100, 162–171. doi: 10.1016/j.ecss.2012.01.012

Chen, H., Zheng, B., Song, J., and Qin, Y. (2011). Correlation between molecular absorption spectral slope ratios and fluorescence humification indices in characterizing CDOM. *Aquat. Sci.* 73, 103–112. doi: 10.1007/s00027-010-0164-5

Chin, Y.-P., Aiken, G., and O'Loughlin, E. (1994). Molecular weight, polydispersity, and spectroscopic properties of aquatic humic substances. *Environ. Sci. Technol.* 28, 1853–1858. doi: 10.1021/es00060a015

Cisek, M., Colao, F., Demetrio, E., Di Cicco, A., Drozdowska, V., Fiorani, L., et al. (2010). Remote and local monitoring of dissolved and suspended fluorescent organic matter off the Svalbard. *J. Optoelectron. Adv. Mater.* 12, 1604–1618.

Coble, P. (1996). Characterization of marine and terrestrial DOM in seawater using excitation-emission matrix spectroscopy. *Mar. Chem.* 51, 325–346. doi: 10.1016/0304-4203(95)00062-3

Cunliffe, M., Upstill-Goddard, R. C., and Murrell, J. C. (2011). Microbiology of aquatic surface microlayers. *FEMS Microbiol. Rev.* 35, 233–246. doi: 10.1111/j.1574-6976.2010.00246.x

Cunliffe, M. A., Engel, S., Frka, S., Gašparović, B., Guitart, C., Murrell, J. C., et al. (2013). Sea surface microlayers: a unified physicochemical and biological perspective of the air–ocean interface. *Prog. Oceanogr.* 109, 104–116. doi: 10.1016/j.pocean.2012.08.004

Darecki, M., Weeks, A., Sagan, S., Kowalczuk, P., and Kaczmarek, S. (2003). Optical characteristics of two contrasting case 2 waters and their influence on remote sensing algorithms. *Cont. Shelf Res.* 23, 237–250. doi: 10.1016/S0278-4343(02)00222-4

Del Veccio, R., and Blough, N. V. (2004). On the origin of the optical properties of humic substances. *Environ. Sci. Technol.* 38, 3885–3891. doi: 10.1021/es049912h

Drozdowska, V., and Fateyeva, N. L. (2013). "Spectrophotometric study of natural Baltic surfactants – results of marine Experiments," in *Hydrobiology in Environment Protection*, eds T. M. Traczewska and B. Hanus-Lorenz (Wrocław: PWR Press), 25–33.

Drozdowska, V., Freda, W., Baszanowska, E., Rudź, K., Darecki, M., Heldt, J. R., et al. (2013). Spectral properties of natural and oil polluted Baltic seawater – results of measurements and modeling. *Eur. Phys. J. Spec. Top.* 222, 1–14. doi: 10.1140/epjst/e2013-01992-x

Drozdowska, V., and Józefowicz, M. (2015). Spectroscopic studies of marine surfactants in the southern Baltic Sea. *Oceanologia* 57, 159–167. doi: 10.1016/j.oceano.2014.12.002

Drozdowska, V., Kowalczuk, P., and Józefowicz, M. (2015). Spectrofluorometric characteristics of fluorescent dissolved organic matter in a surface microlayer in the Southern Baltic coastal waters. *J. Eur. Opt. Soc. Rapid. Publ.* 10:15050. doi: 10.2971/jeos.2015.15050

Drozdowska, V., Wróbel, I., Markuszewski, P., Makuch, P., Raczkowska, A., and Kowalczuk, P. (2017). Study on organic matter fractions in the surface microlayer in the Baltic Sea by spectrophotometric and spectrofluorometric methods. *Ocean Sci.* 13, 633–647. doi: 10.5194/os-13-633-2017

Engel, A., Bange, H. W., Cunliffe, M., Burrows, S. M., Friedrichs, G., Galgani, L., et al. (2017). The ocean's vital skin: toward an integrated understanding of the sea surface microlayer. *Front. Mar. Sci.* 4:165. doi: 10.3389/fmars.2017.00165

Falkowska, L. (1999). Sea surface microlayer: a field evaluation of teflon plate, glass plate and screen sampling techniques. Part 2. Dissolved and suspended matter. *Oceanologia* 41, 223–240.

Galgani, L., Piontek, J., and Engel, A. (2016). Biopolymers form a gelatinous microlayer at the air-sea interface when Arctic sea ice melts. *Sci. Rep.* 6:29465. doi: 10.1038/srep29465

Gao, H., and Zepp, R. G. (1998). Factors influencing photoreactions of dissolved organic matter in a coastal river of the southeastern United States. *Environ. Sci. Technol.* 32, 2940–2946. doi: 10.1021/es9803660

Garrett, W. D. (1965). Collection of slick-forming materials from the sea surface. *Limnol. Oceanogr.* 10, 602–605. doi: 10.4319/lo.1965.10.4.0602

Glatzel, S., Kalbitz, K., Dalva, M., and Moore, T. (2003). Dissolved organic matter properties and their relationship to carbon dioxide efflux from restored peat bogs. *Geoderma* 113, 397–411. doi: 10.1016/S0016-7061(02)00372-5

Goldstone, J. V., Del Vecchio, R., Blough, N. V., and Volker, B. M. (2004). A multicomponent model of chromophoric dissolved organic matter photobleaching. *Photochem. Photobiol.* 80, 52–60. doi: 10.1562/TM-03-17.1

Gonsior, M., Schmitt-Kopplin, P., Stavklint, H., Richardson, S. D., Hertkorn, N., and Bastviken, D. (2014). Changes in dissolved organic matter during the treatment processes of a drinking water plant in Sweden and formation of previously unknown disinfection byproducts. *Environ. Sci. Technol.* 48, 12714–12722. doi: 10.1021/es504349p

Grzybowski, W. (2000). Effect of short-term sunlight irradiation on absorbance spectra of chromophoric organic matter dissolved in coastal and riverine water. *Chemosphere* 40, 1313–1318. doi: 10.1016/S0045-6535(99)00266-0

Hardy, J. T. (1982). The sea-surface microlayer e biology, chemistry and anthropogenic enrichment. *Prog. Oceanogr.* 11, 307–328. doi: 10.1016/0079-6611(82)90001-5

Helms, J. R., Stubbins, A., Ritchie, J. D., Minor, E. C., Kieber, D. J., and Mopper, K. (2008). Absorption spectral slopes and slope ratios as indicators of molecular weight, source, and photobleaching of chromophoric dissolved organic matter. *Limnol. Oceanogr.* 53, 955–969. doi: 10.4319/lo.2008.53.3.0955

Højerslev, N. K. (1974). Inherent and apparent properties of the Baltic, Rep. *Inst. Phys. Oceanogr.* 23:88.

Højerslev, N. K. (1988). Natural occurrences and optical effects of Gelbstoff, Rep. *Inst. Phys. Oceanogr.* 50:30.

Højerslev, N. K. (1989). Surface water-quality studies in the interior marine environment of Denmark. *Limnol. Oceanogr.* 34, 1630–1639. doi: 10.4319/lo.1989.34.8.1630

Hudson, N., Baker, A., and Reynolds, D. (2007). Fluorescence analysis of dissolved organic matter in natural, waste and polluted waters – a review. *River Res. Appl.* 23, 631–649. doi: 10.1002/rra.1005

Huguet, A., Vacher, L., Relexans, S., Saubusse, S., Froidefond, J. M., and Parlanti, E. (2009). Properties of fluorescent dissolved organic matter in the Gironde Estuary. *Org. Geochem.* 40, 706–719. doi: 10.1016/j.orggeochem.2009.03.002

Khundzhua, D. A., Patsaeva, S. V., Terekhova, V. A., and Yuzhakov, V. I. (2013). Spectral characterization of fungal metabolites in aqueous medium with humus substances. *J. Spectrosc.* 2013:538608. doi: 10.1155/2013/538608

Kirk, J. T. O. (1994). *Light and Photosynthesis in Aquatic Ecosystems*. New York, NY: Cambridge University Press. doi: 10.1017/CBO9780511623370

Kowalczuk, P. (1999). Seasonal variability of yellow substance absorption in the surface layer of the Baltic Sea. *J. Geophys. Res. Ocean* 104, 30047–30058. doi: 10.1029/1999JC900198

Kowalczuk, P., Durako, M. J., Young, H., Kahn, A. E., Cooper, W. J., and Gonsior, M. (2009). Characterization of dissolved organic matter fluorescence in the South Atlantic Bight with use of PARAFAC model: interannual variability. *Mar. Chem.* 113, 182–196. doi: 10.1016/j.marchem.2009.01.015

Kowalczuk, P., Stedmon, C. A., and Markager, S. (2006). Modelling absorption by CDOM in the Baltic Sea from season, salinity and chlorophyll. *Mar. Chem.* 101, 1–11. doi: 10.1016/j.marchem.2005.12.005

Kowalczuk, P., Ston-Egiert, J., Cooper, W. J., Whitehead, R. F., and Durako, M. J. (2005). Characterization of chromophoric dissolved organic matter (CDOM) in the Baltic Sea by excitation emission matrix fluorescence spectroscopy. *Mar. Chem.* 96, 273–292. doi: 10.1016/j.marchem.2005.03.002

Kowalczuk, P., Zabłocka, M., Sagan, S., and Kuliński, K. (2010). Fluorescence measured in situ as a proxy of CDOM absorption and DOC concentration in the Baltic Sea. *Oceanologia* 52, 431–471. doi: 10.5697/oc.52-3.431

Kuliński, K., Hammer, K., Schneider, B., and Schulz-Bull, D. (2016). Remineralization of terrestrial dissolved organic carbon in the Baltic Sea. *Mar. Chem.* 181, 10–17. doi: 10.1016/j.marchem.2016.03.002

Kurata, N., Kate Vella, K., Hamilton, B., Shivji, M., Soloviev, A., Matt, S., et al. (2016). Surfactant-associated bacteria in the near-surface layer of the ocean. *Sci. Rep.* 6:19123. doi: 10.1038/srep19123

Lepparanta, M., and Myrberg, K. (2009). *Physical Oceanography of the Baltic Sea*. Heidelberg: Springer, 378. doi: 10.1007/978-3-540-79703-6

Liss, P. S., and Duce, R. A. (1997). *The Sea Surface and Global Change*. Cambridge: Cambridge University Press. doi: 10.1017/CBO9780511525025

Loiselle, S. A., Bracchini, L., Dattilo, A. M., Ricci, M., Tognazzi, A., Cózar, A., et al. (2009). The optical characterization of chromophoric dissolved organic matter using wavelength distribution of absorption spectral slopes. *Limnol. Oceanogr.* 54, 590–597. doi: 10.4319/lo.2009.54.2.0590

McKnight, D. M., Boyer, E. W., Westerhoff, P. K., Doran, P. T., Kulbe, T., and Andersen, D. T. (2001). Spectrofluorometric characterization of dissolved organic matter for indication of precursor organic material and aromaticity. *Limnol. Oceanogr.* 46, 38–48. doi: 10.4319/lo.2001.46.1.0038

Miller, W. L., and Zepp, R. G. (1995). Photochemical production of dissolved inorganic carbon from terrestrial organic matter: significance to the oceanic organic carbon cycle. *Geophys. Res. Lett.* 22, 417–420. doi: 10.1029/94GL03344

Moran, M. A., Sheldon, W. M. Jr., and Zepp, R. G. (2000). Carbon loss and optical property changes during long-term photochemical and biological degradation of estuarine dissolved organic matter. *Limnol. Oceanogr.* 45, 1254–1264. doi: 10.4319/lo.2000.45.6.1254

Murphy, K. R., Butler, K. D., Spencer, R. G. M., Stedmon, C. A., Boehme, J. R., and Aiken, G. R. (2010). Measurement of dissolved organic matter fluorescence in aquatic environments: an interlaboratory comparison. *Environ. Sci. Technol.* 44, 9405–9412. doi: 10.1021/es102362t

Olszewski, J., Sagan, S., and Darecki, M. (1992). Spatial and temporal changes in some optical parameters in the southern Baltic. *Oceanologia* 33, 87–103.

Osburn, C. L., O'Sullivan, D. W., and Boyd, T. J. (2009). Increases in the longwave photobleaching of chromophoric dissolved organic matter in coastal waters. *Limnol. Oceanogr.* 54, 145–159. doi: 10.4319/lo.2009.54.1.0145

Parlanti, E., Worz, K., Geoffroy, L., and Lamotte, M. (2000). Dissolved organic matter fluorescence spectroscopy as a tool to estimate biological activity in a coastal zone submitted to anthropogenic inputs. *Org. Geochem.* 31, 1765–1781. doi: 10.1016/S0146-6380(00)00124-8

Pastuszak, M., Stålnacke, P., Pawlikowski, K., and Witek, Z. (2012). Response of Polish rivers (Vistula, Oder) to reduced pressure from point sources and agriculture during the transition period (1988–2008). *J. Mar. Syst.* 94, 157–173. doi: 10.1002/etc.3519

Sieburth, J. M. (1983). "Microbiological and organic-chemical processes in the surface and mixed layers," in *Air-Sea Exchange of Gases and Particles*, eds P. S. Liss and W. G. N. Slinn (Hingham, MA: Reidel Publishers Co), 121–172.

Stedmon, C. A., Markager, S., and Bro, R. (2003). Tracing dissolved organic matter in aquatic environments using a new approach to fluorescence spectroscopy. *Mar. Chem.* 82, 239–254. doi: 10.1021/acs.est.8b02648

Stedmon, C. A., Markager, S., and Kaas, H. (2000). Optical properties and signatures of chromophoric dissolved organic matter (CDOM) in Danish coastal waters. *Estuar. Coast. Shelf Sci.* 51, 267–278. doi: 10.1006/ecss.2000.0645

Szymczycha, B., Winogradow, A., Karol Kuliński, K., Koziorowska, K., and Pempkowiak, J. (2017). Diurnal and seasonal DOC and POC variability in the land-locked sea. *Oceanologia* 59, 379–388. doi: 10.1016/j.oceano.2017.03.008

Tilstone, G. H., Angel-Benavides, I. M., Pradhan, Y., Shutler, J. D., Groom, S., and Sathyendranath, S. (2010). An assessment of chlorophyll-a algorithms available for SeaWiFS in coastal and open areas of the Bay of Bengal and Arabian Sea. *Remote Sens. Environ.* 115, 2277–2291. doi: 10.1016/j.rse.2011.04.028

Timko, S., Maydanov, A., Pittelli, S. L., Conte, M. H., Cooper, W. J., Koch, B. P., et al. (2015). Depth-dependent photodegradation of marine dissolved organic matter. *Front. Mar. Sci.* 2:66. doi: 10.3389/fmars.2015.00066

Twardowski, M. S., Boss, E., Sullivan, J. M., and Donaghay, P. L. (2004). Modeling the spectra shape of absorption by chromophoric dissolved organic matter. *Mar. Chem.* 89, 69–88. doi: 10.1016/j.marchem.2004.02.008

Williams, C. J., Yamashita, Y., Wilson, H. F., Jaffé, R., and Xenopoulos, M. A. (2010). Unraveling the role of land use and microbial activity in shaping dissolved organic matter characteristics in stream ecosystems. *Limnol. Oceanogr.* 55, 1159–1171. doi: 10.4319/lo.2010.55.3.1159

Williamson, C. E. (1995). What role does UV-B radiation play in freshwater ecosystems? *Limnol. Oceanogr.* 40, 386–392. doi: 10.4319/lo.1995.40.2.0386

Wilson, H. F., and Xenopoulos, M. A. (2009). Effects of agricultural land use on the composition of fluvial dissolved organic matter. *Nat. Geosci.* 2, 37–41. doi: 10.1038/ngeo391

Zepp, R. G., Callaghan, T. V., and Erickson, D. J. (1998). Effects of enhanced solar ultraviolet radiation on biogeochemical cycles. *J. Photochem. Photobiol. B Biol.* 46, 69–82. doi: 10.1007/BF02986960

Zhang, Y., Liu, X., Osburn, C. L., Wang, M., Qin, B., and Zhou, Y. (2013). Photobleaching response of different sources of chromophoric dissolved organic matter exposed to natural solar radiation using absorption and excitation–emission matrix spectra. *PLoS One* 8:e77515. doi: 10.1371/journal.pone.0077515

Zhou, X. L., and Mopper, K. (1997). Photochemical production of low-molecular-weight carbonyl compounds in seawater and surface microlayer and their air-sea exchange. *Mar. Chem.* 56, 201–213. doi: 10.1016/S0304-4203(96)00076-X

Zsolnay, A., Baigar, E., Jimnez, M., Steinweg, B., and Saccomandi, F. (1999). Differentiating with fluorescence spectroscopy the sources of dissolved organic matter in soils subjected to drying. *Chemosphere* 38, 45–50. doi: 10.1016/S0045-6535(98)00166-0

Conflict of Interest Statement: The authors declare that the research was conducted in the absence of any commercial or financial relationships that could be construed as a potential conflict of interest.